Electronic Supplementary Material (ESI) for Journal of Materials Chemistry B.

Supporting Information

Designing compartmentalized hydrogel microparticles for cell encapsulation and scalable 3D cell culture

*Yen-Chun Lu, Wei Song, Duo An, Beum Jun Kim, Robert Schwartz, Mingming Wu and Minglin Ma**

Table of Contents:

1. Materials and methods

2. Supplementary experimental results and figures

3. Supplementary references

1. Materials and methods

Measurement of tumor microtissue growth in microparticles

The microtissue size was defined as the mean of the longest dimension and the shortest dimension of the microtissue and measured by ImageJ. [1, 2] When the microtissues stopped growing, the size was defined as the maximum size. At each time point, the microtissue size was presented as a percentage of the maximum size. Typically, the MCF-10A microtissues reached the maximum size in 5 days and the MDA-MB-231 microtissues reached the maximum in 10 days (Figure 3, c).

Cell Viability Assessment

The cell viability was characterized with live/dead acetoxymethyl ester of calcein (calcein AM)/ethidium homodimer-1 (EthD-1) dyes (Life technologies). Two methods were used to assess the cell viability. In the first method, the cells were stained directly in microparticles; in the second method, the cells were recovered from the microparticles before the staining. The microparticles with cells or cells obtained from microparticles were incubated with 20 μM calcein AM and 14 μM EthD-1 for 10-20 mins.

Tumor microtissue harvest from microparticles

We obtained the microtissues from the microparticles by dissolving the alginate outer layer using a 50 mM EDTA solution with 10mM HEPES (pH 7.4). Before dissolving alginate, these microparticles were washed by PBS three times.

Microscopy and image analysis

The microparticles was observed and imaged by an EVOS AMF4300 imaging system. The fluorescent images were obtained through the EVOS inverted fluorescent microscope. The collagen fibers in the microparticles were imaged by reflectance confocal microscope (Zeiss LSM710 confocal microscope operated by ZEN software v. 2010, Carl Zeiss).

Albumin ELISA

The rat albumin concentrations were determined using a sandwich enzyme-linked immunosorbant assays (Bethyl Lab) with horseradish peroxidase and 3,3¢,5,5¢-tetramethylbenzidine (TMB, Fitzgerald Industries) as a substrate.

Statistics analysis

The numeric data were presented as mean ± SE. The data were compared through one-way analysis of variance (ANOVA).

Seeding the microparticles in microwells

The microparticles with a predetermined number were poured onto the microwells placed in a well of a 6-well plate. The plate was placed on a 360 degree multi-purpose shaker for ~ 30 minutes. A small fraction of the particles that were trapped in the inter-well space were manually removed using a pipet.

Viscosity Measurement

The viscosity of alginate solution and Matrigel cell suspension were measured by Viscometery (A&D SV10 Vibro Viscometer). The viscometer was firstly calibrated by deionized water before measuring the samples.

2. Supplementary experimental results and figures

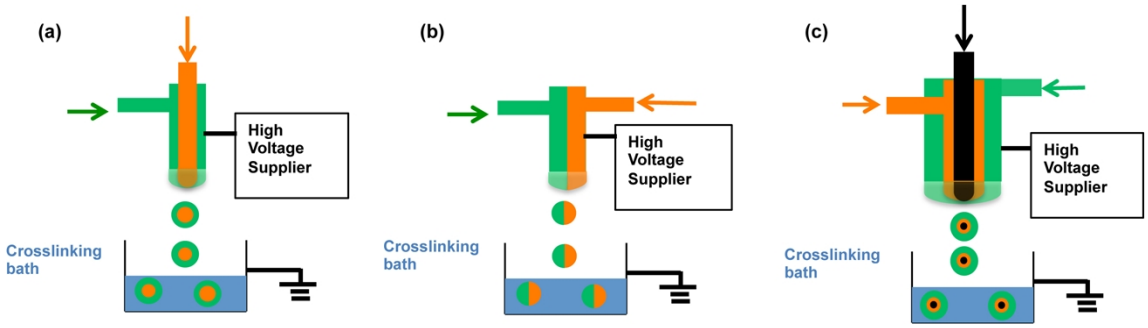

Figure S1. Schematics for the multi-fluidic electrospraying to produce the three different configurations of structured alginate hydrogel microparticles. (a) Double-layer; the nozzle has an inner tube (I.D. ~200 μm, O.D. ~400 μm) and an outer tube (I.D. ~750 μm, O.D. ~1200 μm) (b) Side-by-side; the nozzle has two connected tubes (I.D. ~200 μm, O.D. ~400 μm) (c) Triple layer microparticles. The nozzle has three concentric tubes (I.D. ~150 μm, O.D. ~300 μm; I.D. ~600 μm, O.D. ~900 μm; I.D. ~1,100 μm, O.D. ~1,400 μm)

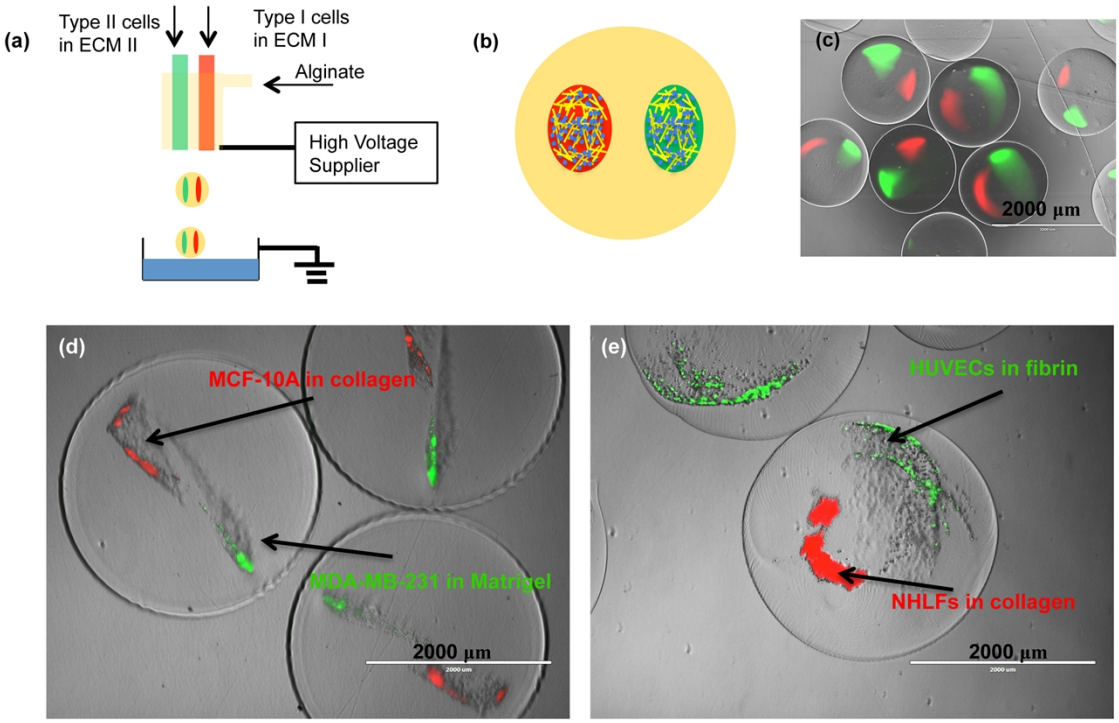

Figure S2. Hydrogel particles with an alginate outer layer and two ECM cores for cell encapsulation. (a, b) Schematics of the setup and the microparticles. (c) The two cores visualized by fluorescent alginates (red and green). (d) The MCF-10A (red) with collagen and MDA-MB-231 (green) in Matrigel encapsulated in the double-core microparticles. (e) HUVECs (green) in fibrin and NHLF cells (red) with collagen encapsulated in the double-core microparticles.

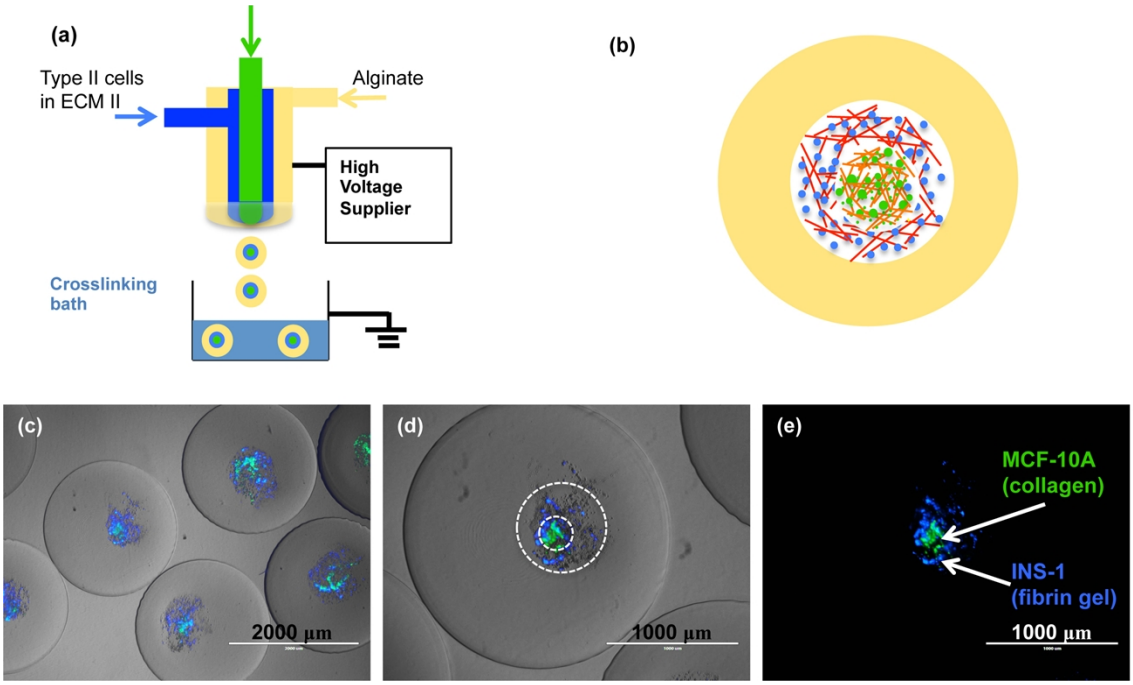

Figure S3. Triple-layer concentric hydrogel particles with an alginate outer layer and two ECM inner layers. (a, b) Schematics of the setup and the microparticles. (c-e) The MCF-10A (green) in collagen matrix as the innermost layer, surrounded by INS-1 cells (blue, stained with Hoechst) in fibrin within the alginate outermost layer.

Configuration	Extracellular matrix component used in this study	Cell lines used in this study	Potential applications
Double-layer	Fibrin, collagen and Matrigel	HUVECs, NHLF, MDA-MB-231, MCF-10A, hepatocyte, small intestinal organoids	Microtissue production, co-culture, liver model, stem cell culturing
Double-core	Fibrin, collagen and Matrigel	HUVECs, NHLF, MDA-MB-231, MCF-10A	Paracrine co-culture
Triple-layer	Fibrin, collagen	MCF10A, INS-1	Paracrine co-culture, cell migration

Table S1. A summary of different microparticle configurations.

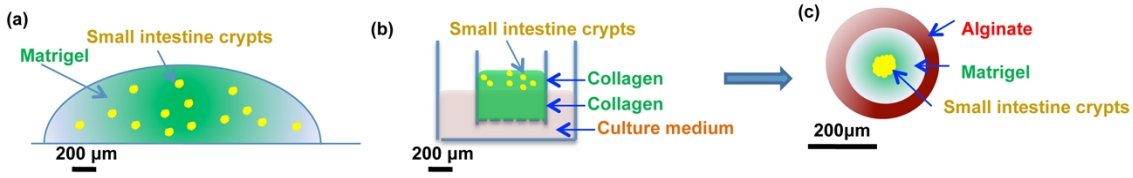

Figure S4. Schematics of different culturing methods for the small intestinal crypts. (a) The crypts cultured in a Matrigel droplet. (b) The crypts embedded in collagen gel near air-liquid interface in first dish that was inserted in a second dish containing medium as a "dish-in-dish" configuration. (c) The crypts grown with Matrigel in microparticles. The microparticles have increased surface-to-volume ratio and reduced diffusion distance as compared with the bulk hydrogel.

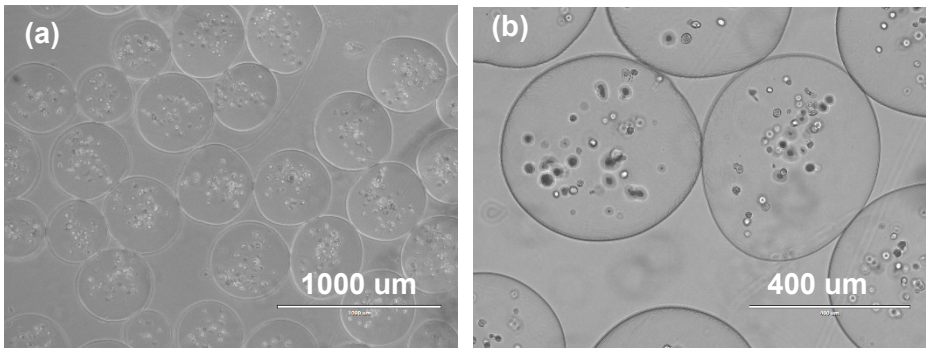

Figure S5. The MDA-MB-231 cells encapsulated in alginate alone microparticles (day 13) did not proliferate.

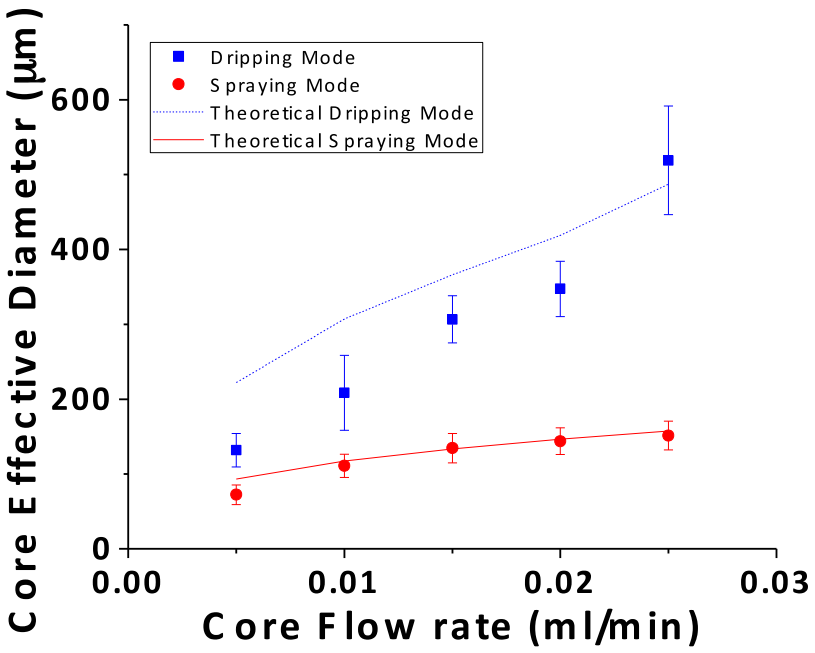

Figure S6. Controlling of the size of the ECM inner (core) layer in the double-layer microparticles. The plots show the core size as a function of the core flow rate given a fixed flow rate of 0.45 ml-min^{-1} for the outer, shell fluid. The experimental data (in dots) were compared with theoretical values (in lines) in both dripping and spraying modes. The effective diameter (D') of the core was approximated as the average of the longest and shortest dimensions determined by ImageJ. The theoretical values were derived as the following:

The shell flow rate $Q_{shell} = \frac{4}{3}\pi(\frac{D}{2} - \frac{D'}{2})^3 \Big/ \Delta t$ (Equation S1)

where D is the overall diameter of the particles, and approximately 420 μm in the spraying mode. In the dripping mode, D was measured for each batch of particles.

The core flow rate $Q_{core} = \frac{4}{3}\pi(\frac{D'}{2})^3 \Big/ \Delta t$. (Equation S2)

The ratio of the two flow rates $\frac{Q_{shell}}{Q_{core}} = (\frac{D}{D'})^3 - 1$ (Equation S3)

The theoretical effective diameter was obtained by re-arrangement.

$$D' = D \Big/ \sqrt[3]{\left(\frac{Q_{shell}}{Q_{core}}\right) - 1} \quad \text{(Equation S4)}$$

The theoretical values and experimental data were consistent for the spraying mode. However, in the dripping mode the ECM core might diffuse into the alginate shell before the gelation occurred (since the dripping was typically much slower than the spraying), leading to smaller core sizes than the theoretical values.

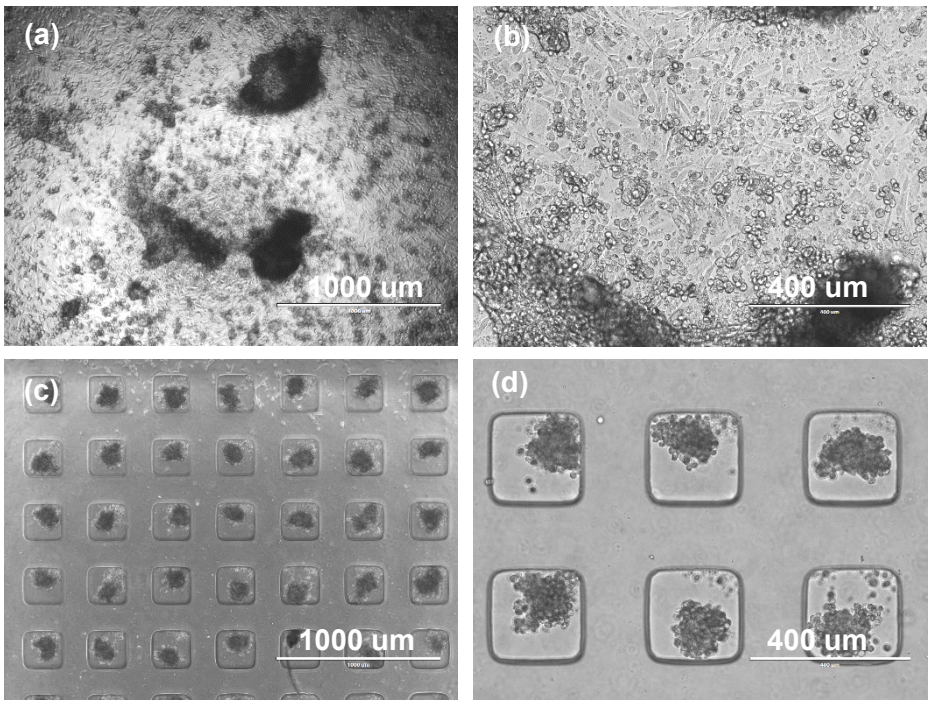

Figure S7. Assessment of microtissue formation of MDA-MB-231 cells embedded in Matrigel^{TM} (a, b) and seeded (with Matrigel) in microwells (c, d). The Matrigel was diluted to 16.7% using culture medium, similar to the case of microparticles. After 16 days culturing, the cells in the bulk gel randomly formed cell aggregates of several different sizes, while in the PDMS microwells the cells formed better aggregates, similar to previous studies.[3] However, the aggregates formed in the microwells seemed structurally loose, as compared to those formed in the microparticles.

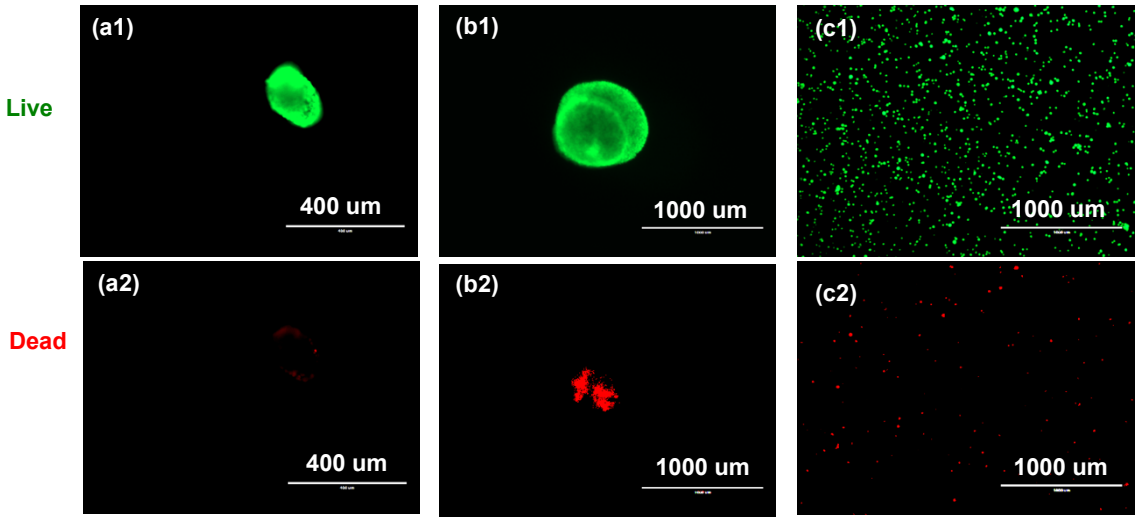

Figure S8. The viability assessment for MDA-MB-231 microtissue with two different sizes (200 μm and 700 μm). (a) The viability of MDA-MB-231 microtissue with size around 200 μm; (b, c) The live/dead staining results of a 700 μm microtissue. In (b), the microtissue was stained directly, while in (c) the microtissue was broken into single cells before staining to show individual live/dead cells.

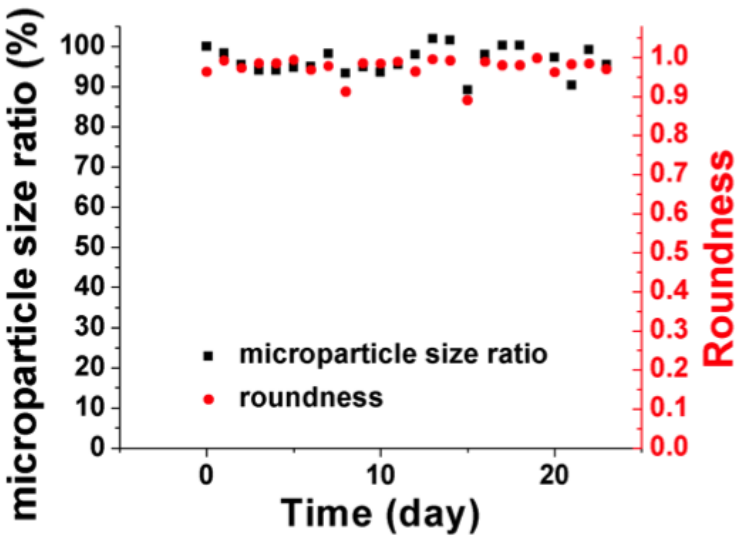

Figure S9. The morphometric characterization of a representative alginate microparticle over time. The size (diameter) and roundness of the alginate microparticle (with cells) were measured from Day 0 to Day 24. (The roundness is defined by $\frac{4 * (area)}{\pi * (major\ axis)^2}$ calculated through ImageJ)

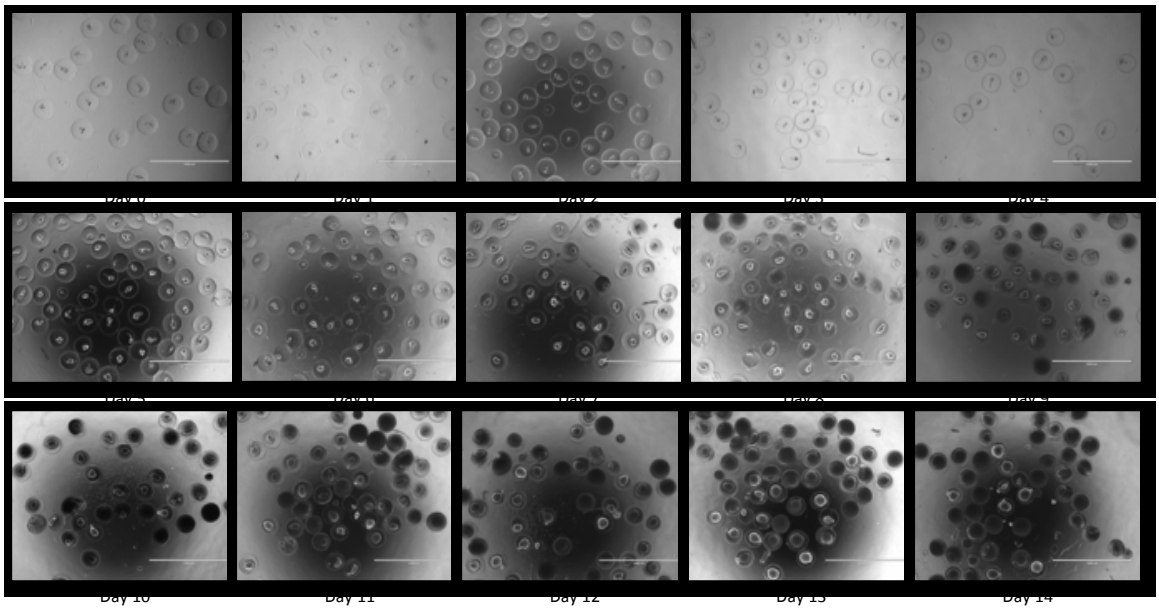

Figure S10. Ins-1 cells grow in alginate/Matrigel double-layer microparticles over 2 weeks. Note the darkening and breakage of microparticle. (All images are at the same magnification and the scale bars are 2 mm.)

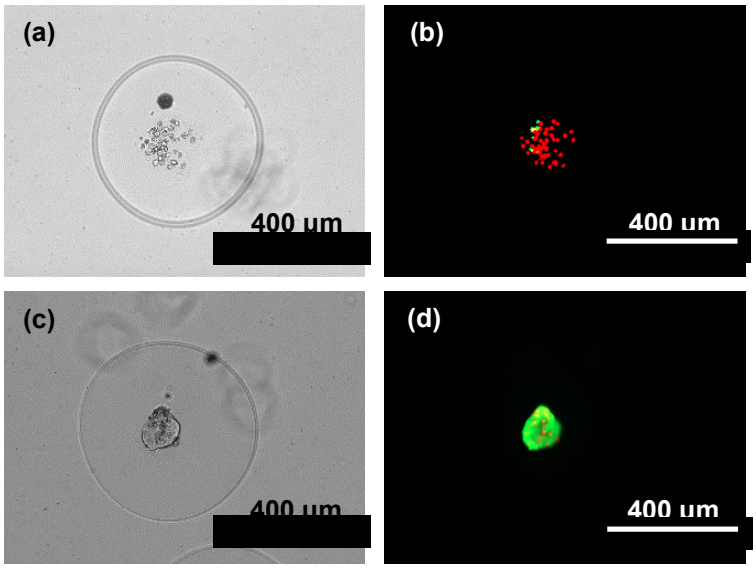

Figure S11. (a, b) Rat hepatocytes encapsulated alone in the Matrigel-supported microparticles: the hepatocytes appeared loosely dispersed (a) and mostly dead as indicated by live (green) / dead (red) staining on day 2. (c, d) Rat hepatocytes co-encapsulated with mouse 3T3-J2 stromal cells were better aggregated (c) and mostly alive (d).

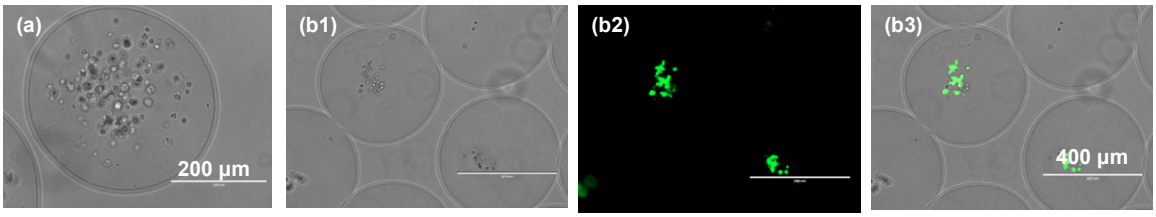

Figure S12. HUVECs with GFP expression were encapsulated in alginate alone particles and alginate/fibrin double-layer ones. (a) The HUVECs in alginate alone particles were mostly dead after two days as indicated by no GFP expression. (b) The HUVECs in fibrin gel were still mostly alive after 10 days. (All scale bars in b1, b2 and b3 are 400 μm.)

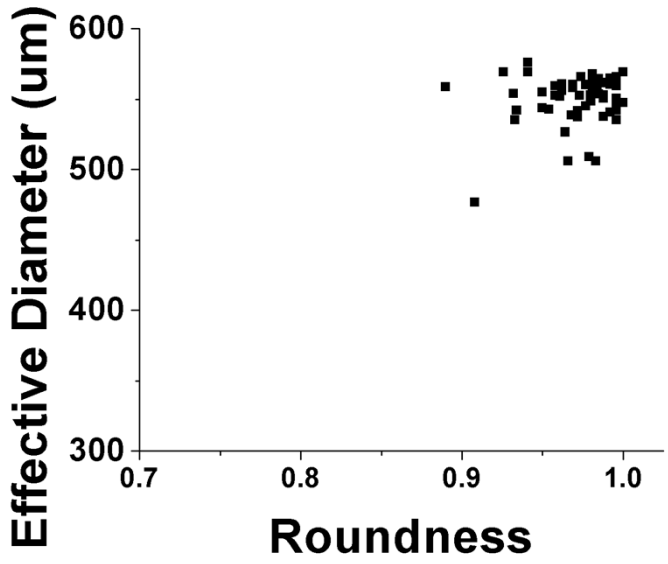

Figure S13. The morphometric characterization of alginate microparticles. All the alginate microparticles (n=65) were analyzed through ImageJ. The effective diameters (average of major axis and minor axis) of this batch microparticles varied from 540 to 560 μm except 4 smaller ones less than 510 μm. In addition, the roundness analysis $\frac{4 * (area)}{\pi * (major\ axis)^2}$ of the microparticles revealed that most of particles were close to perfect spheres.

Supplementary Reference

1. C. A. Schneider, W. S. Rasband and K. W. Eliceiri, *Nat Methods*, 2012, **9**, 671-675.
2. S. M. Hartig, *Current protocols in molecular biology / edited by Frederick M. Ausubel ... [et al.]*, 2013, **Chapter 14**, Unit14 15.
3. M. Vinci, S. Gowan, F. Boxall, L. Patterson, M. Zimmermann, W. Court, C. Lomas, M. Mendiola, D. Hardisson and S. A. Eccles, *BMC Biol*, 2012, **10**, 29.